DELAMINATION DETECTION IN COMPOSITE BEAM USING MODIFIED AIS AlGORITHM WITH EXPERIMENTAL VALIDATION

B. Mohebbi[1*], F. Abbasidoust[1], M.M Ettefagh[1], H. Biglari[1]

[1]*Mechanical Engineering Department, University of Tabriz, Tabriz, Iran.*
[*]*Mohebbi_behzad@yahoo.com*

Keywords: Composite Beam, Delamination Detection, Vibration Analysis, Artificial Intelligence Algorithms.

Abstract

In this study vibration-based delamination detection is achieved using artificial immune system (AIS) method. The approach is based upon mimicking immune recognition mechanisms that possess features such as adaptation, evolution, and immune learning. The delamination location and length in composite beam identified as an optimization problem. The cost function based on differences between analytical or experimental natural frequencies and predicted natural frequencies by AIS method. Analytical natural frequencies of delaminated beam obtained from Euler-Bernoulli beam theory with constrained delamination mode. Errors of predicted location and length are 2.16% and 0.1968% respectively, using the AIS algorithm. To investigate the accuracy of the proposed method some experimental results were extracted. A laser vibrometer used to found out natural frequencies change in delaminated CFRP composite beam case study. The average values of location and length errors are 18.7% and 9.8% respectively, between AIS method and experiment.

1. Introduction

Damage detection in composite structures is an important because of their increasingly use in the construction of aerospace, civil, marine, automotive and other high performance structures. Delamination is one of the major damage modes in laminated composites due to their weak interlaminar strength. Delaminations may arise during fabrication or service-induced strains, such as incomplete wetting, air entrapment, impact of foreign objects, exposure to unusual level of excitation, etc [1]. Delaminations are embedded within the composite structures so they may not be visible or barely visible on the surface but they can reduce stiffness and strength of the structures [2]. Damage detection in structures is one of the common topics that have received growing interest in research communities [3]. While a number of damage detection and localization methods have been proposed in this paper, a novel damage diagnosing method based on AIS algorithm has been developed, which incorporates several major characteristics of the natural immune system [4]. The damage patterns are represented by feature vectors that are extracted from the structure's dynamic response measurements. In our method the possible changes in the natural frequencies of the structure are utilized as a feature vector because frequencies can be measured more easily than other vibration parameters such as mode shapes on the other hand they are less critically affected by experimental errors.

The selective and adaptive features of the proposed algorithm allow the AIS to evolve its antibodies towards the goal of minimizing the described cost function. The performance of the

presented structure damage detector has been validated using a model of damaged (delaminated) structure. For modeling the delaminated-beam composite structure an analytical model of a delaminated cantilever beam is utilized and natural frequencies are obtained through numerical methods [5]. The identification of the delamination location and length in the cantilever beam is formulated as an optimization problem [5]. Also the frequencies has been obtained by experimental method for one of our case studies, both these frequencies obtained by experiment and theory have been used as the AIS algorithm's input, the results show that experiments validate the integrity of our method.

2. Natural and artificial immune systems

The biological immune system is a complex adaptive system that has evolved in vertebrates to protect them from invading pathogens. The biological immune system can be envisioned as a multilayer protection system, where each layer provides different types of defense mechanisms for detection, recognition and responses. Thus, three main layers include the anatomic barrier, innate immunity (nonspecific) and adaptive immunity (specific). Innate immunity and adaptive immunity are inter-linked and influence each other. Once adaptive immunity recognizes the presence of an invader, it triggers two types of responses humoral immunity and cell-mediated (cellular) immunity, which act in a sequential fation.

Innate immunity is directed against any pathogen. If an invading pathogen escapes the innate defenses, then the body can launch an adaptive or specific response against a particular type of foreign agent [4].

3. AIS-based structure damage detection

The fault detection system is designed using concepts derived from the natural immune system. The component correspondence between the natural immune system and the AIS-based structure damage detection method is cited in the next subsection. The AIS algorithm in our implementation is used to damage detection by defining an cost function *C(.,.)*,

$$C(X,L) = \sum_{i=1}^{4} \text{abs}(f_i - f_i^*) \tag{1}$$

Which should be minimized based upon the calculated and corresponding to unknown natural frequencies. In Eq.(1) X is the location of the delamination from one end, and L is the length of the delamination. f_i's are the first four natural frequencies, which are functions of X and L, and are calculated from the delaminated-beam model, f_i^*'s are the first four natural frequencies which are applied to our delamination detection system as inputs. A zero cost value indicates an exact match between the corresponding frequencies. In this section, the modified immune optimization algorithm is discussed.

3.1. Immune terminologies and representations

This section defines the major components and parameters used in the AIS algorithm.
Antigen: each peak of the function to be optimized.
Antibody: an individual of the population represented as a real-valued attribute string in the Euclidean shape-space.
Fitness: affinity between the antibody and Ag, an index to measure the goodness of the antibody.
Affinity: Euclidean distance between two antibodies.
Clone: offspring antibodies that are identical to the parent antibody.
Mutated clone: a clone that has undergone somatic mutation.
Memory cell: the antibodies with higher fitness and antigenic affinities are selected to become memory cells with long life spans.

Negative selection: if there is any antibodies in memory cells, whose affinity with Ab_i is higher than a defined limit this Ab_i is discarded.

3.2. The algorithm

Step1: Generate *n* antibodies randomly within the range (0 , 1).

$$P = \{p_1, p_2, p_3, ..., p_n\}$$
$$p_1 = (x_{11}, x_{12}, x_{13}, ..., x_{1d})$$
$$p_2 = (x_{21}, x_{22}, x_{23}, ..., x_{2d})$$
$$\vdots$$
$$p_n = (x_{n1}, x_{n2}, x_{n3}, ..., x_{nd})$$

Step2: Generate *nc* of clones for each antibody Ab_i in the population.

$$N_C = n \times n_c$$
$$C = \{C_1, C_2, C_3, ..., C_n\} = \{q_1, q_2, q_3, q_4, q_5, ..., q_{N_c}\}$$
$$C_1 = \overbrace{\{p_1, p_1, p_1, ...p_1\}}^{n_c}$$
$$C_2 = \{p_2, p_2, p_2, ...p_2\}$$
$$\vdots$$
$$C_n = \{p_n, p_n, p_n, ...p_n\}$$

Step3: Mutate each clone. The mutation rate has inverse relationship with the number of iteration of parent invariance.

$$\begin{cases} c_i^* = q_i + \mu \times rand & \text{for } i = 2,3,4,...,nc, nc+2, nc+3, ..., 2nc, 2nc+2, ... \\ c_i^* = q_i & \text{for } i = 1, nc+1, 2nc+1, 3nc+1, ... \end{cases} \qquad C^* = \{c_1^*, c_2^*, c_3^*, ..., c_{N_c}^*\}$$

Rand is a number between (0 , 1).

Step4: Decode the antibodies within the domain of variables of function and determine the fitness of all the individuals in the population.

Step5: For each clone, select only the one with the highest fitness to generate a new population.

Step6: recognizing the answers and enter them in memory cell. If a member of population does not change in N_{mem} iterations, it will be saved in memory cell.

Step7: using negative selection to replace random member instead of self antibodies.

Step8: Repeat Step 2 to Step 5 until stopping criteria's is satisfied.

- Maximum number of iterations allowed.
- Maximum number of iterations that algorithm can continue without finding a new answer.
- Maximum number of answers that algorithm can find.

4. Delaminated composite beam modeling

In order to detect delamination locations/size, it's necessary to obtain the analytical solution to the vibration of composite beams with different Delaminations.

The delaminated beam considered as 3n+1 Euler-Bernoulli classical beam (with Li>>hi) [6, 7] which are connected at the delamination boundaries, where n is number of delaminations (geometry of beam in shown in Fig.1) in the present paper, the 'constrain mode' are considered. Using Euler-Bernoulli beam theory, the governing equations for intact beam section are [8]:

$$D_i \frac{\partial^4 \omega_i}{\partial x^4} + \rho_i A_i \frac{\partial^2 \omega_i}{\partial t^2} = 0 \qquad (1)$$

Where D_i is the reduced bending stiffness of the i-th beam, ρ_i is the density of material, A_i is the cross sectional area; *x* is the axial coordinate and *t* is the time. The reduced bending stiffness is as follows [9]:

$$D_i = D^i{}_{11} - \frac{(B^i{}_{11})^2}{(A^i{}_{11})} \tag{2}$$

Where

$$D^{(i)}{}_{11} = \frac{b}{3}\sum_{k=1}^{n_i}(\overline{Q^k{}_{11}})_k(z_k{}^3 - z_{k-1}{}^3) \tag{3}$$

$$B^{(i)}{}_{11} = \frac{b}{2}\sum_{k=1}^{n_i}(\overline{Q^k{}_{11}})_k(z_k{}^2 - z_{k-1}{}^2) \tag{4}$$

$$A^{(i)}{}_{11} = b\sum_{k=1}^{n_i}(\overline{Q^k{}_{11}})_k(z_k - z_{k-1}) \tag{5}$$

$$\overline{Q^k}_{11} = Q^k{}_{11}\cos^4\phi + 2\left(Q^k{}_{12} + 2Q^k{}_{44}\right)\sin^2\phi\cos^2\phi + Q^k{}_{22}\sin^4\phi \tag{6}$$

$$Q_{11} = \frac{E_{11}}{1-\nu_{12}\nu_{21}} \qquad Q_{22} = \frac{E_{22}}{1-\nu_{21}\nu_{12}} \qquad Q_{66} = G_{12} \qquad \nu_{12} = \frac{\nu_{12}E_{22}}{E_{11}} \tag{7}$$

Where $A^{(i)}{}_{11}$ is the extensional stiffness, $D^{(i)}{}_{11}$ is the bending stiffness, $B^{(i)}{}_{11}$ is the coupling stiffness, $\overline{Q^k}_{11}$ is the coefficient stiffness of the lamina, b is the width, E_{11} and E_{22} are the longitudinal and transverse young's moduli , respectively, ν_{12} and ν_{21} are the longitudinal and transverse Poisson's ratio, G_{12} is the in-plane shear modulus ,respectively, ϕ is the angle of K-th lamina orientation where 2K and 2k-1 are the locations of the K-th lamina with respect to the midplane of i-th beam.

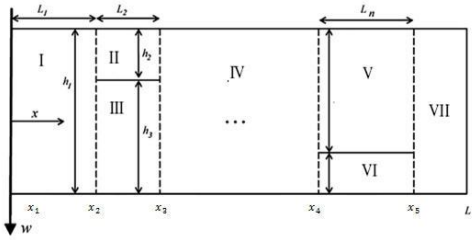

Figure 1. delaminated beam geometry

The equation (1) is valid for intact beam. According to the concept of constrained model the delaminated Sections are forced to vibrate together, therefore governing equation for beam 1-4 are:

$$D_1\frac{\partial^4\omega_{\mathrm{I}}}{\partial x^4} + \rho_1 A_1\frac{\partial^2\omega_{\mathrm{I}}}{\partial t^2} = 0 \tag{8}$$

$$(D_3 + D_2)\frac{\partial^4\omega_{\mathrm{II}}}{\partial x^4} + (\rho_2 A_2 + \rho_3 A_3)\frac{\partial^2\omega_{\mathrm{II}}}{\partial t^2} = 0 \tag{9}$$

$$D_4 \frac{\partial^4 \omega_{1V}}{\partial x^4} + \rho_4 A_4 \frac{\partial^2 \omega_{1V}}{\partial t^2} = 0 \tag{10}$$

For free vibrations, the response can be assumed as follows:

$$w_i(x,t) = W_i(x)\sin(\omega t) \tag{11}$$

Where ω denotes natural frequency and $W_i(x)$ is the mode shape of i-th beam section substituting Eq.(11) into Eq.(1) and eliminating the trivial solution $\sin(\omega t)=0$ one can obtain the general solution of the differential equation (1) as:

$$W_i(x) = C_i \cos(\lambda_i \frac{x}{L}) + S_i \sin(\lambda_i \frac{x}{L}) + CH_i \cosh(\lambda_i \frac{x}{L}) + SH_i \sinh(\lambda_i \frac{x}{L}) \tag{12}$$

Where

$$\lambda_i^4 = \frac{\omega^2 \rho_i A_i}{D_i} L^4 \tag{13}$$

Unknown coefficients C_i, S_i, SH_i, CH_i can be determined from boundary and continuity conditions. The continuity conditions for the deflection, slope, shear (Q) and bending moments (M) at $x=x_2$ are as follows (see Fig. 2) [6]:

$$W_{\mathrm{I}} = W_{\mathrm{II}} \tag{14}$$

$$W_{\mathrm{I}}' = W_{\mathrm{II}}' \tag{15}$$

$$D_1 W_{\mathrm{I}}''' = (D_2 + D_3) W_{\mathrm{II}}''' \tag{16}$$

$$M_1 = M_2 + M_3 - \frac{1}{2} P_2 (H_1 - H_2) + \frac{1}{2} P_3 (H_1 - H_3) \tag{17}$$

Where

$$Q_i = -D_i W_i''' \qquad M_i = -D_i W'' \tag{18}$$

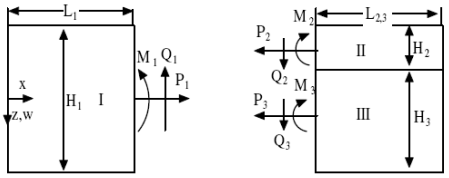

Figure 2.bending moment and shear force at the delamination boundary

The axial forces Pi can be established from compatibility between stretching/shortening of the delaminated layers and axial equilibrium which results

$$\frac{P_3 L_2}{A^3_{11}} - \frac{P_2 L_2}{A^2_{11}} = (W_1'(x_2) - W_4'(x_3)) \frac{H_1}{2} \tag{19}$$

$$P_1 = P_2 + P_3 = 0 \tag{20}$$

We can obtain continuity equations for bending moment with substituting E.q (19) and (20) into Eq. (17)

$$D_1 W_1''(x_2) + \frac{H^2_1}{L_2} \frac{A_{11}^{(2)} A^{(3)}_{11}}{A_{11}^{(2)} + A^{(3)}_{11}} (W_1'(x_2) - W_4'(x_3)) - (D_2 + D_3) D_1 W''_2(x_2) \tag{21}$$

The boundary and continuity conditions provide a coefficient matrix with 8n+4 orders where n is the number of delaminations. A non trivial solution for the coefficients exists only when determinant of the coefficient matrix vanishes.

5 .Numerical results

We study present method using a cantilever beam with a single Delamination, which was studied by Shen and Grady [10]. The beam is made of T300/934 graphite/epoxy cantilever beam with a [0◦/90◦] 2s stacking sequence. The dimensions of the 8-ply beam are 127×12.7×1.016 mm^3. The material properties for the lamina are: E_{11} = 134 GPa, E_{22} = 10.3 GPa, G_{12} =5 GPa, v_{12} = 0.33 and $\rho = 1.48 \times 10^3$ kg/m^3. All delaminations are at the midspan and the lengths are 25.4 mm, 50.8 mm, 76.2 mm and 101.6 mm the first four frequencies calculated for the composite beam with cantilever boundary conditions, (h_2/h_1=0.5) are shown in Table 1. There is a good agreement between the frequencies calculated by the present model and experimental [10] analytical [11] and FEM results [10]. The input natural frequencies are shown in Table 2.

Table 3 presents predicted test points of Delamination in AIS. The prediction error is calculated from the following formula:

$$\%\text{Error} = \frac{\text{predicted value} - \text{actual value}}{\text{actual value}} \times 100\,(\%) \tag{22}$$

Delamination length (mm)	Present (Hz)	Shu and Della [17]	Shen and Grady [15]	Luo and Hangud [18]
0.0	82.01	81.88	82.04	81.86
25.4	80.02	80.47	80.13	81.84
50.8	74.45	75.36	75.29	76.81
76.2	65.14	66.14	66.94	67.64
101.6	54.81	55.67	57.24	56.95

Table1. Primary frequencies for cantilever composite beam

Test point no.	Desired value (mm)		Input natural frequencies(Hz)			
	X	L	1st	2nd	3rd	4th
1	50.8	25.4	80.0288	481.6375	879.6543	1.2174e+003
2	38.1	50.8	74.4523	447.4076	851.9948	1.9024e+003
3	25.4	76.2	65.1414	385.3599	752.4364	1.5040e+003
4	12.7	101.6	54.8101	308.8741	713.5140	1.3996e+003

Table2. The input natural frequencies

Using Artificial Immune system					
Prediction (mm)		Error (mm)		Error (%)	
X	L	X	L	X	L
50.3	25.4	-0.5	0	-0.98	0
39.3	50.7	1.2	- 0.1	3.14	-0.1968
25.4	76.2	0	0	0	0
12.7	101.6	0	0	0	0
Average		0.7	-0.1	2.16	0.1968

Table3. Predicted values by AIS

6. Experimental setup

We carried out two experiments Fig.4 to investigate the accuracy of the present model and measurements errors. In first experiment, the first three natural frequencies of an intact beam are measured and results are used to update the material properties of our model with AIS method. Optimization targets were: E_{11}, E_{22}, G_{12}, v_{12} and ρ.

In the second experiment we measured natural frequencies of the laminated beam with delamination length of 25.4 mm and in the midspan of the beam with (h_2/h_1=0.5) then we use these frequencies to predict delamination location (X) and length (L).

In each case the beam was excited by a mini shaker (JZK Sinocera) at the distance of 127 mm from the fixed end. The dynamic response of the beam was measured using laser vibrometer (Ometron VH 300) targeted at 47mm from the fixed end. The response measurements were acquired using signal analyzer (Pulse 2827 B&K) and the frequency response of the beam was acquired using FFT analyzer (3107 B&K). The frequency response of the beam is shown in Fig 3. The results of natural frequency measurements for intact experimental cases are shown in Table 4 and updated material properties are shown in Table 5. After frequency measurements, three lowest natural frequencies are used for fault diagnosis, and the delamination location and length are estimated. The estimation results are shown in Table 6.

Test case	Location (mm)	Length (mm)	natural frequencies(Hz)		
			1st	2nd	3rd
delaminated	50.8	25.4	64.8	349	1050
intact			68	417	1221

Table 4.mesured natural frequencies for experimental cases

	E_{11}(GPa)	E_{22}(GPa)	G_{12}(GPa)	v_{12}	ρ (kg/m3)
Initial properties	134	10.3	5	0.33	1.48×10^3
Updated Properties	110.55	11.86	4.6	0.28	1.8×10^3

Table 5.updated properties using AIS algorithm

Exact value(mm)		Prediction (mm)		Error (mm)		Error (%)	
X	L	X	L	X	L	X	L
50.8	25.4	60.3	27.9	9.5	2.5	18.7	9.8

Table 6.actual and estimation delamination length and location for experimental case

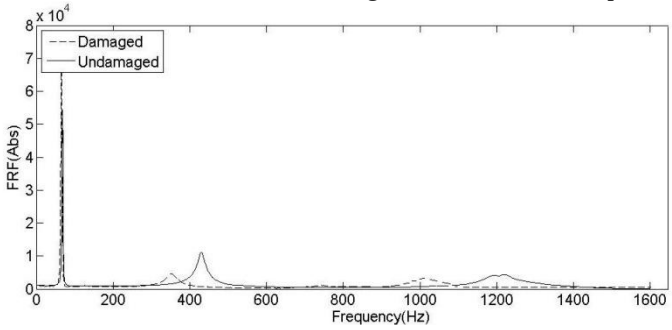

Figure 3. Frequency response for delaminated and intact beam obtained by FFT analyzer (3107 B&K)

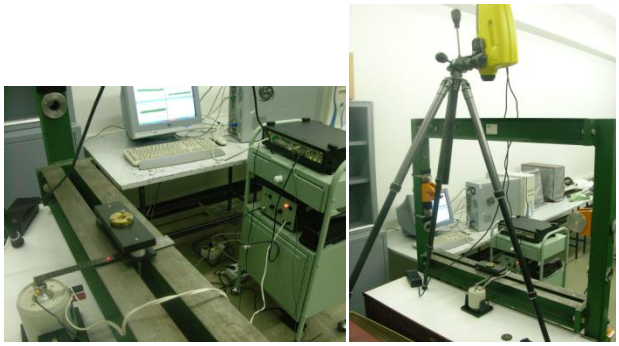

Figure 4. Experimental setup

7. Conclusion

For the improvement of reliability, safety and efficiency advanced methods of supervision, fault detection and fault diagnosis become increasingly important in many engineering systems. The components of the AIS such as its representation, affinity function, and immune process are tailored for the damage detection. The evolution and immune learning algorithms make it possible for the damage detector to generate a high quality memory cell set for recognizing various structure damages. The average values of location and length prediction errors are 2.16% and 0.1968% for the AIS method, respectively. The effectiveness of this method is approved by experimental results, the prediction values for location and length errors are 18.7% and 9.8%, respectively. The proposed model has the ability to be used for analysis of complex structures with different kinds of damages.

8. References

[1] D. Chakraborty, Artificial neural network based delamination prediction in laminated composites, *Materials and Design*, 26, pp. 1–7, (2005).

[2] Garg, A.C., Delamination – a damage mode in composite structures, *Engrg. Frac. Mech*, 29, pp.557–584, (1988).

[3] S. W. Doebling, C. R. Farrar, M. B. Prime, and D. W. Shevitz, Damage Identification and Health Monitoring of Structural and Mechanical Systems From Changes in Their Vibration Characteristics: A Literature Review, *Los Alamos National Laboratory Report LA-13070-MS*, (1996).

[4] D.Dasgupta, Advances in Artificial Immune Systems, *Computational intelligence magazine*, IEEE, pp. 40-49, (2006).

[5] J. Timmis, A.N.W. Hone, T. Stibor, E. Clark,Theoretical advances in artificial immune systems, *Theoretical Computer Science*, (2008).

[6] C.N. Della, D. Shu, Vibration of delaminated composite laminates: a review, *Applied Mechanics Reviews*, 60, pp.1–20, (2007).

[7] D. Shu, C.N. Della, Free vibration analysis of composite beams with two non-overlapping delaminations, *International Journal of Mechanical Sciences*, 46, pp.509–526, (2004).

[8]Mujumdar, P.M., Suryanarayan, S, Flexural vibrations of beams with delaminations, *J. Sound Vib*, 125, pp.441–461,(1982).

[9] J.N. Reddy, Mechanics of Laminated Composite Plates, *CRC Press*, (1997).

[10] Shen, M.-H.H., Grady, J.E., Free vibrations of delaminated beams, *AIAA J*, 30, pp.1361–1370,(1992).

[11] Luo, H., Hanagud, S., Dynamics of delaminated beams, *Int. J. Solids Struct*, 37, pp.1501–1519,(2000).